

NUMERICAL ANALYSIS ON FAILURE PRESSURE OF PIPELINES WITH
MULTI-CORRODED REGION

NG YEW KEONG

Report submitted in partial fulfillment of requirements
for award of the Degree of
Bachelor of Mechanical Engineering

Faculty of Mechanical Engineering
UNIVERSITI MALAYSIA PAHANG

JUNE 2013

ABSTRACT

The underground gas pipeline is vulnerable which can explode any time. The percentage of the pipeline fails due to the pressure may cause fatal destruction. Hence, the predictions of pipeline burst pressure in the early stage are very important in order to provide assessment for future inspection, repair and replacement activities. This thesis is to study the effect of multiple corrosion defects on failure pressure for API X42 steel and validate the results with available design codes. The project implicates analysis by using MSC Patran 2008 r1 software as a pre-processor and MSC Marc 2008 r1 software as a solver. Half of the pipe was simulated by fully applying symmetrical condition. The pipe is modeled in 3-D with outer diameter 381 mm, wall thickness of 17.5 mm and different defect parameter. In this analysis, SMCS and von Mises stress used to predict the failure pressure. The result shows that the failure pressure increases when the distance between defect increases but decreases when the defect length increases. SMCS always shows a higher value compared to von Mises. The design codes applied only when the distance between defect is small enough that multiple defects acts as a single defect. Meanwhile, value of FEA is the highest among all the design codes.

ABSTRAK

Saluran paip gas bawah tanah terdedah yang boleh meletup bila-bila masa. Peratusan perancangan gagal kerana tekanan boleh menyebabkan kerosakan maut. Oleh itu, ramalan-ramalan saluran paip tekanan pecah pada peringkat awal adalah amat penting dalam usaha untuk memberikan penilaian untuk pemeriksaan masa depan, pembaikan dan aktiviti penggantian. Karya ini adalah untuk mengkaji kesan pelbagai kecacatan hakisan pada tekanan kegagalan API X42 keluli dan mengesahkan keputusan dengan kod reka bentuk boleh didapati. Projek ini membabitkan analisis dengan menggunakan perisian Patran 2008 r1 MSC sebagai pra-pemproses dan Marc 2008 perisian MSC r1 sebagai penyelesai. Separuh daripada paip adalah simulasi dengan menggunakan sepenuhnya keadaan simetri. Paip ini dimodelkan dalam 3-D dengan diameter luar 381 mm, ketebalan dinding sebanyak 17.5 mm dan parameter kecacatan yang berbeza. Dalam analisis ini, SMC dan von Mises tekanan digunakan untuk meramalkan tekanan kegagalan. Hasilnya menunjukkan bahawa tekanan kegagalan meningkat apabila jarak antara kenaikan kecacatan tetapi berkurangan apabila kenaikan panjang kecacatan. SMC sentiasa menunjukkan nilai yang lebih tinggi berbanding dengan von Mises. Kod reka bentuk digunakan hanya apabila jarak antara kecacatan cukup kecil bahawa pelbagai kecacatan bertindak sebagai kecacatan tunggal. Sementara itu, nilai FEA adalah yang tertinggi di kalangan semua kod reka bentuk.

TABLE OF CONTENTS

	Page
EXAMINER’S DECLARATION	ii
SUPERVISOR’S DECLARATION	iii
STUDENT’S DECLARATION	iv
DEDICATIONS	v
ACKNOWLEDGEMENTS	vi
ABSTRACT	vii
ABSTRAK	viii
TABLE OF CONTENTS	ix
LIST OF TABLES	xiii
LIST OF FIGURES	xiv
LIST OF SYMBOLS	xx
LIST OF ABBREVIATIONS	xxi
 CHAPTER 1 INTRODUCTION	
 1.1 Introduction	1
1.2 Problem Statement	2
1.3 Objectives	2
1.4 Scopes	2
 CHAPTER 2 LITERATURE REVIEW	
 2.1 Introduction	3
2.2 Pipelines issues in Malaysia	3
2.3 Material	5
2.4 Type of defects	7
2.4.1 Corrosion	7
2.4.2 Dents and gouges	8
2.5 Type of corrosion	9

2.5.1	Uniform attacks	10
2.5.2	Galvanic or two metal corrosion	10
2.5.3	Pitting corrosion	11
2.5.4	Erosion corrosion	12
2.5.5	Microbiologically-influenced corrosion (MIC)	13
2.5.6	Intergranular corrosion	13
2.6	Internal and external corrosion	14
2.7	Fundamental and theory equations	16
2.7.1	Engineering stress and strain	16
2.7.2	Modulus of elasticity	16
2.7.3	True stress and strain	17
2.7.4	Relationship between Engineering Stress-Strain and True Stress-Strain	17
2.7.5	Relationship between true stress and true strain	17
2.8	Stress in pressurised cylinders	18
2.8.1	Hoop stress	18
2.8.2	Radial stress	20
2.8.3	Longitudinal stress	20
2.9	Material and specimen geometry	20
2.10	Experimental results	21
2.11	Finite element analysis	23
2.11.1	FE model and analysis	22
2.11.2	Comparison with experimental results	24
2.12	Evaluation of failure pressure	25
2.12.1	Stress modified critical strain (SMCS)	25
2.12.2	Design codes	26
2.12.3	PCORCC	27

CHAPTER 3 METHODOLOGY

3.1	Introduction	29
3.2	Flowchart	29
3.3	Flowchart description	31
3.3.1	Literature review	31
3.3.2	Specimen preparation	31
3.3.3	Material	34
3.3.4	Machining process	34
3.3.5	Notched dimension	38
3.3.6	Spectrometry analysis	39
3.3.7	Uniaxial tension test	40
3.3.8	Experiment apparatus	40

3.3.9	Tensile specimen	41
3.3.10	Experiment procedures	43
3.3.11	Measurement of final diameter of rupture specimens	43
3.3.12	Analysis of tensile test data	45
3.3.13	Development of failure criteria equation	47
3.4	FE Analysis	48
3.4.1	Structure modelling	49
3.4.2	Simulation procedure	50
3.5	Simulation	57
3.6	Gantt Chart	58

CHAPTER 4 RESULTS AND DISCUSSION

4.1	Introduction	59
4.2	Result	60
4.2.1	Comparison of failure pressure between SMCS and von Mises for different distance between defects with same defect length of 100 mm	61
4.2.2	Comparison of failure pressure between SMCS and von Mises for different distance between defects with same defect length of 200 mm	66
4.2.3	Comparison of failure pressure between SMCS and von Mises for different distance between defects with same defect length of 300 mm	71
4.2.4	Comparison of failure pressure for different defect length	76
4.2.5	Comparison of failure pressure between SMCS and von Mises for different defect length with same distance between defects of 5 mm	77
4.2.6	Comparison of failure pressure between SMCS and von Mises for different defect length with same distance between defects of 50 mm	80
4.2.7	Comparison of failure pressure between SMCS and von Mises for different defect length with same distance between defects of 100 mm	83
4.2.8	Comparison of failure pressure for different distance between defects	86
4.2.9	Comparison of failure pressure between design codes and FEA for different defect length with same distance between defects of 5 mm	87
4.2.10	Comparison of failure pressure between PCORCC and FEA for different defect length with same distance between defects of 5 mm	89
4.3	Stress contour	90

CHAPTER 5 CONCLUSION AND RECOMMENDATION

5.1	Introduction	94
5.2	Conclusion	94
5.3	Recommendation	95

REFERENCES	96
-------------------	----

APPENDICES

A	Gantt Chart	98
B	Engineering drawing of specimens	99
C	Chemical composition of material	103

LIST OF TABLES

Table No.	Title	Page
2.1	Physical properties of the API 5L line pipe	6
2.2	Chemical properties of the API 5L line pipe	7
3.1	Physical and chemical properties of API X42	34
3.2	Machining parameters	36
3.3	Experiment parameters	43
3.4	Dimension parameters	49
3.5	Material data for API X42	56
4.1	Summarise of failure pressure of different defect dimensions	60
4.2	Comparison of failure pressure between SMCS and von Mises to different distance between defects with same defect length of 100 mm	61
4.3	Comparison of failure pressure between SMCS and von Mises to different distance between defects with same defect length of 200 mm	66
4.4	Comparison of pressure pressure between SMCS and von Mises to different distance between defects with same defect length of 300 mm	71
4.5	Comparison of SMCS and von Mises to different defect length with the same distance between defects of 5 mm	77
4.6	Comparison of SMCS and von Mises to different defect length with the same distance between defects of 50 mm	81
4.7	Comparison of SMCS and von Mises to different defect length with the same distance between defects of 100 mm	84
4.8	Comparison of failure pressure between design codes and FEA to different defect length with same distance between defects of 5mm	88
4.9	Comparison of failure pressure between PCORCC and FEA to different defect length with same distance between defects of	89

LIST OF FIGURES

Figure No.	Title	Page
2.1	Existing and planned gas pipelines in Malaysia	4
2.2	Location of SOGT and SSGP	5
2.3	Corroded pipeline	8
2.4	Defects of dents and gouges	9
2.5	Generalized corrosion	10
2.6	Galvanic corrosion	11
2.7	The rust indicates the pitting is occurring	12
2.8	Erosion corrosion	12
2.9	Microbiologically-influenced corrosion	13
2.10	Intergranular corrosion	14
2.11	Internal corrosion	15
2.12	External corrosion	15
2.13	Hoop stress	19
2.14	Cylinder subjected to both internal and external pressure	19
2.15	Schematic illustration of tensile bars	21
2.16	Experimental engineering stress-strain data	22
2.17	True stress-strain for API X65	22
2.18	FE meshes for notched tensile bars: (a) R0.2, (b) R1.5 and (c) R3	23
2.19	Comparison of experimental engineering stress-strain data	24
2.20	Comparison of experimental engineering stress-strain data	24
3.1	Flowchart	30
3.2	Smooth tensile bar	32

3.3	1.5R notched tensile bar	32
3.4	3R notched tensile bar	33
3.5	6R notched tensile bar	33
3.6	Hydraulic bend saw	37
3.7	Conventional lathe machine	37
3.8	Turning process	37
3.9	Tool, HSS create the notched part	38
3.10	Transformation of raw material to specimen	38
3.11	Profile projector to measure the notched dimension	39
3.12	Optical emission spectrometry	39
3.13	Instron 3369 Universal Testing machine	40
3.14	1.5R notched specimen	41
3.15	3.0R notched specimen	42
3.16	6.0R notched specimen	42
3.17	Smooth specimen	42
3.18	Microscope Marvision MM 320-Mahr	44
3.19	Quadra-Chek 300	44
3.20	Engineering stress-strain for API X42	46
3.21	True stress-strain for API X42	47
3.22	Simulation flowchart	48
3.23	Full pipeline with multiple defects	49
3.24	Closed up view of multiple defects	50
3.25	Configuration before starting MSC Patran	50
3.26	Points and lines created	51

3.27	Surface and normal forces in x-axis	52
3.28	Full design of a half of the pipe	52
3.29	Multi defects on pipeline	53
3.30	Meshing	54
3.31	Boundaries conditions that applied	54
3.32	Reduce integration	55
3.33	True strain and true stress values	55
3.34	Material update	56
3.35	Setting of analysis	57
4.1	Graph of SMCS failure pressure versus distance between defects of 100 mm defect length	62
4.2	Graph of SMCS failure pressure versus $(W/l)^2$ of 100 mm defect length	62
4.3	Graph of von Mises failure pressure versus distance between defects of 100 mm defect length	63
4.4	Graph of von Mises failure pressure versus $(W/l)^2$ of 100 mm defect length	63
4.5	Graph of comparison between SMCS and Von Mises for failure pressure versus $(W/l)^2$ of 100 mm defect length	64
4.6	SMCS stress distribution of 100 mm distance between defects	65
4.7	von Mises stress distribution of 100 mm distance between defects	65
4.8	Graph of SMCS failure pressure versus distance between defects of 200 mm defect length	67
4.9	Graph of SMCS failure pressure versus $(W/l)^2$ of 200 mm	67

	defect length	
4.10	Graph of von Mises failure pressure versus distance between defects of 200 mm defect length	68
4.11	Graph of von Mises failure pressure versus $(W/l)^2$ of 200 mm defect length	68
4.12	Graph of comparison between SMCS and von Mises of failure pressure versus $(W/l)^2$ of 200 mm defect length	69
4.13	SMCS stress distribution of 200 mm distance between defects	70
4.14	von Mises stress distribution of 200 mm distance between defects	70
4.15	Graph of SMCS failure pressure versus distance between defects of 300 mm defect length	72
4.16	Graph of SMCS failure pressure versus $(W/l)^2$ of 300 mm defect length	72
4.17	Graph of von Mises failure pressure versus distance between defects of 300 mm defect length	73
4.18	Graph of von Mises failure pressure versus $(W/l)^2$ of 300 mm defect length	73
4.19	Graph of comparison between SMCS and von Mises of failure pressure versus $(W/l)^2$ of 300 mm defect length	74
4.20	SMCS stress distribution of 300 mm distance between defects	75
4.21	von Mises stress distribution of 300 mm distance between defects	75
4.22	Graph of SMCS failure pressure versus $(W/l)^2$ for three different defect length	76
4.23	Graph of von Mises failure pressure versus $(W/l)^2$ for three different defect length	76
4.24	Graph of SMCS failure pressure versus defect length of 5 mm distance between defects	78

4.25	Graph of von Mises failure pressure versus defect length of 5 mm distance between defects	78
4.26	Graph of comparison between SMCS and von Mises of failure pressure versus defect length of 5 mm distance between defects	79
4.27	SMCS stress distribution of 100 mm defect length	79
4.28	von Mises stress distribution of 100 mm defect length	80
4.29	Graph of SMCS burst pressure versus defect length of 50 mm distance between defects	81
4.30	Graph of Von Mises burst pressure versus defect length of 50 mm distance between defects	81
4.31	Graph of comparison between SMCS and Von Mises of burst pressure versus defect length of 50 mm distance between defects	82
4.32	SMCS stress distribution of 200 mm defect length	82
4.33	von Mises stress distribution of 200 mm defect length	83
4.34	Graph of SMCS burst pressure versus defect length of 100 mm distance between defects	84
4.35	Graph of Von Mises burst pressure versus defect length of 100 mm distance between defects	84
4.36	Graph of comparison between SMCS and Von Mises of burst pressure versus defect length of 100 mm distance between defects	85
4.37	SMCS stress distribution of 300 mm defect length	85
4.38	von Mises stress distribution of 300 mm defect length	86
4.39	Graph of SMCS burst pressure versus defect length for different distance between defects	86
4.40	Graph of Von Mises burst pressure versus defect length for different distance between defects	87
4.41	Graph of comparison between design codes and FEA of burst pressure versus defect length	88
4.42	Graph of comparison between PCOPCC and FEA of burst	89

	pressure versus defect length	
4.43	SMCS stress contour at different pressure level	90
4.44	von Mises stress contour at different pressure level	92

LIST OF SYMBOLS

M	Bulging stress magnification factor
D	Outer diameter of the pipe
t	Wall thickness
σ_y	Yield strength of the material
σ_u	Ultimate tensile strength
l	Length of defect
d	Defect depth
W	Distance between defects
ε_f	Equivalent fracture strain
ε_f^*	Equivalent fracture strain for smooth specimen
σ_m	Hydraulic stress
σ_e	Equivalent stress
K	Strength coefficient
n	Strength hardening exponent

LIST OF ABBREVIATIONS

2D	Two Dimension
3D	Three Dimension
API	American Petroleum Institute
ASME	American Society of Mechanical Engineer
ASTM	American Society for Testing and Materials
FEA	Finite Element Analysis
HSS	High Speed Steel
SMCS	Stress Modified Critical Strain
VGM	Void Grow Model

CHAPTER 1

INTRODUCTION

1.1 BACKGROUND

Nowadays, offshore and onshore pipelines are the highest capacity and the safest means of gas or oil transmission in the world. Trans Thailand-Malaysia Gas Pipeline (TTM) is a gas pipeline linking suppliers in Malaysia to consumers in Thailand. It is a part of the Trans-ASEAN Gas Pipeline project to transport and process natural gas.

However, underground gas pipelines are often damaged due to surrounding and third-party accidents throughout the years as well as increasing of ages. The most common defects in the pipelines are corrosion and dents. Hence, the probability of gas leaking or bursting of the pipeline has increased. The aging pipelines also known as underground time bombs can cause fatal destruction.

Failure due to internal and external corrosion defects has been a major concern in maintaining pipeline integrity. As a pipeline ages, it can be affected by a range of corrosion mechanism, which lead to a reduction in its structural integrity and eventual failure. Corrosion occurs as individual pits, colonies of pits, general wall-thickness reduction, or in combinations. For the pipe with colonies of pits, they begin to interact reducing the burst strength of the pipe as the distance between two corrosion pits decreases.

Naturally, the corrosion started at the point of cracking. The dents and gouges also participate in the formation of corrosion. However, the outer corroded surface of pipelines with desired size and orientation is quite difficult to get in a short time.

Therefore, the artificial defects with desired shape is created to have a different type of analysis. The determination of burst pressure for underground gas pipelines is critical to prevent accidents. Throughout this research the effect of multiple corrosion defects on failure pressure and validation of results with available design codes can be determined.

1.2 PROBLEM STATEMENT

The underground gas pipeline is vulnerable which can explode any time. The defects on the surface of the pipeline further increase the danger. The percentage of the pipeline fails due to the pressure may cause fatal destruction. The main defects that caused the pipes to fail are corrosion and third party such as dents and gouges. The dimension of the defects plays important role in the pipeline failure. The depth, width, and length are vital to determine the burst pressure. The effect of these parameters on burst pressure must be analyzed in order to predict the failure of the pipes. The multiple corroded defects aligned longitudinally are located at outer surface of the pipe. The corroded defects are made artificially with desired dimension for simulation.

1.3 OBJECTIVES

The objectives of the study are as follows:

- i. To study the effect of multiple corrosion defects on failure pressure.
- ii. To validate the results with available design codes.

1.4 SCOPES

The scopes of the study are as follows:

- i. Machining: tensile test specimens
- ii. Spectrometry analysis
- iii. Uniaxial tension test according to ASTM E8 for smooth and notched specimens
- iv. Development of failure criteria
- v. Structural modelling: model the pipe with multi corroded region using MSC Patran software
- vi. Analysis: A 3D Non-linear FEA using MSC Marc software

CHAPTER 2

LITERATURE REVIEW

2.1 INTRODUCTION

This chapter will briefly explain about the properties, material, design, failure, and cause of failure in the pipeline. The sources are taken from journals, articles, and books. Besides, the information about the software that will be used also included in this chapter. The purpose of literature review is to provide information on previous research and that can help to run this project smoothly. All this information is important before furthering to the analysis and study later.

2.2 PIPELINES ISSUES IN MALAYSIA

Underground pipelines transport large quantities of product from the source to the marketplace. The first oil pipeline, which measured at 175 km in length and 152 mm in diameter, was laid from Bradford to Allentown, Pennsylvania in 1879 (Thompson and Beavers, 2006). Since the late 1920s, virtually all oil and gas pipelines have been made of welded steel.

Malaysia has the one of the most extensive natural gas pipeline networks in Asia (EIA, 2011). The Peninsular Gas Utilization (PGU) project expanded the natural gas transmission infrastructure in Peninsular Malaysia. The PGU project is an integral part of Malaysia's economic development plan and involves the construction and installation of facilities for production, processing, and transmission of gas to customers throughout peninsular Malaysia (Gas Technology, 1998). The PGU pipeline project, with a total distance of 1,688 km is supplying Peninsular Malaysia and Singapore with a total of 56

million cubic meters a day, with an additional standby capacity of 21 million cubic meters a day (APERC, 2000). The figure 2.1 shows the major existing and planned domestic gas pipelines in Malaysia.

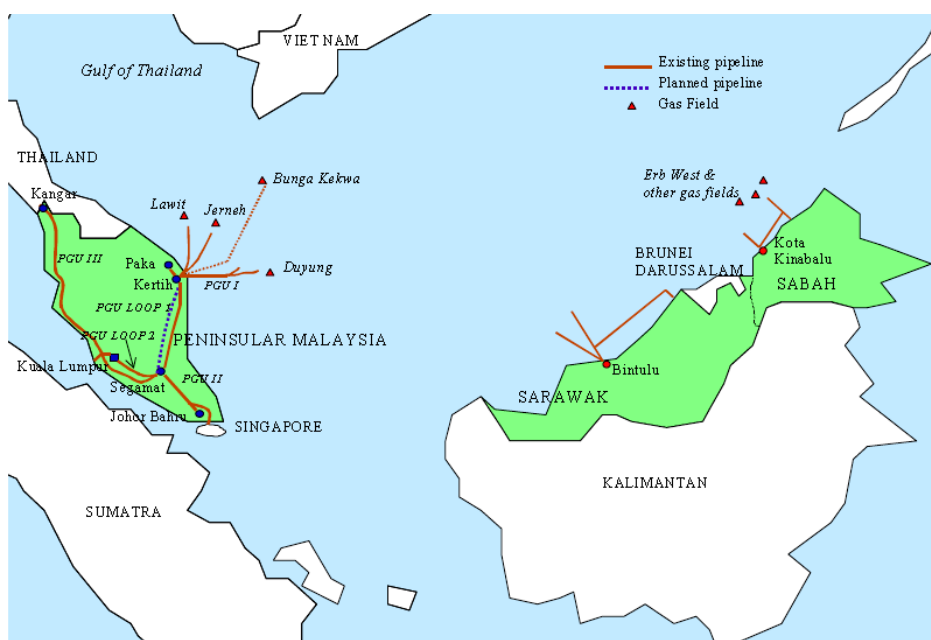


Figure 2.1: Existing and planned gas pipelines in Malaysia

Source: APERC (2000)

The RM4.6 billion Sabah-Sarawak gas pipeline project linking Kimanis in Sabah and Bintulu in Sarawak, expected to be completed by the end of 2013, will be successful as the North-South Expressway (PLUS) linking the Peninsular Malaysia states (New Straits Times, 2011). This project would transport gas from the Sabah Oil and Gas Terminal in Kimanis to customers in Sabah and Petronas LNG complex in Bintulu. Once operational, the terminal will be able to receive, store, and export up to 300,000 bbl/d of crude oil, as well as receive, process, compress, and transport up to 1.25 Bcf/d of gas produced from the Gumusut/Kakap, Kinabalu Deep and East, Keabangan, and Malikai field (Pipelines In International, 2012; EIA, 2011; Petronas, 2012). The 512 km, 36 inch diameter Sabah Sarawak Gas Pipeline (SSGP) will transport 750 MMcf/d of gas from the Sabah Oil and Gas Terminal (SOGT) to the Petronas LNG Complex. Figure 2.2 shows the location of SOGT and SSGP. It's being

constructed using API 5L X70 steel grade pipe, with a thickness of 14,17, and 20 mm, and will have a design pressure of 96 bar.

Malaysia was the third exporter of LNG in the world after Qatar and Indonesia in 2010, exporting over 1 Tcf of LNG, which accounted for 10 percent of total world LNG exports (EIA, 2011). The Bintulu LNG complex in Sarawak is the main hub for Malaysia's natural gas industry. SOGT will supply gas for domestic use in Sabah, largely for a new electric power plant slated for completion in 2014. A reported 500,000 cubic feet per day will be piped to Bintulu complex to be exported as LNG.



Figure 2.2 Location of SOGT and SSGP

Source: Sedia (2012)

2.3 MATERIAL

Most of the pipe used for oil and gas pipelines, particularly in the United States, is either seamless or longitudinal welded pipe. But spiral weld pipe has been used increasingly in oil and gas service in many areas of the world (Kennedy, 1993). Pipe furnished to API Spec 5L may be heat treated using one of several processes: rolled, normalized, normalized and tempered, quenched and tempered, subcritically stress-

relieved, or subcritically age-hardened. Heat treating processes are used to modify the steel's characteristic to give it specific physical properties. The Table 2.1 shows the physical properties of the API 5L line pipe.

Table 2.1: Physical properties of the API 5L line pipe

API 5L Grade	Yield Strength min. (MPa)	Tensile Strength min. (MPa)	Yield to Tensile Ratio (max.)	Elongation min. %
A	206.84	330.95	0.93	28
B	241.32	413.68	0.93	23
X42	289.58	413.68	0.93	23
X46	317.16	434.37	0.93	22
X52	358.53	455.05	0.93	21
X56	386.11	489.53	0.93	19
X60	413.68	517.11	0.93	19
X65	448.16	530.90	0.93	18
X70	482.63	565.37	0.93	17
X80	551.58	620.53	0.93	16

Source: Woodco USA

The chemical composition of steels is varied to provide specific properties. API specifications give a detailed listing of the amount of each element that can be contained in a given grade of steel used for line pipe. Carbon is a key component in all steels. The amount of carbon affects the strength, ductility, and other physical properties of steel. Maximum carbon content ranges from 0.21%-0.31%, depending on the grade of steel used and the method of pipe manufacture. In general, the amount of manganese required in line pipe steel increases as the grade (strength) increases. For instance, the maximum manganese in Grade A pipe is 0.90% and the maximum content in Grade X70 is 1.60% (Kennedy, 1993). The chemical properties of the API 5L line pipe indicates in Table 2.2.

Table 2.2: Chemical properties of the API 5L line pipe

Grade & Class	Carbon, Max	Manganese, Max	Phosphorus		Sulfur, Max	Titanium, Max
			Min	Max		
A25, C1 I	0.21	0.60		0.030	0.030	
A25, C1 II	0.21	0.60	0.045	0.080	0.030	
A	0.22	0.90		0.030	0.030	
B	0.28	1.20		0.030	0.030	0.04
X42	0.28	1.30		0.030	0.030	0.04
X46, X52, X56	0.28	1.40		0.030	0.030	0.04
X60	0.28	1.40		0.030	0.030	0.04
X65, X70	0.28	1.40		0.030	0.030	0.06

Source: API (2004)

2.4 TYPES OF DEFECT

The possibility defects in the pipeline can be occurred during manufacturing, transportation, fabrication and installation, and occur both due to deterioration and due to external interference. The main factor cause of damage and failures in transmission pipelines in Western Europe and North America is external interference (Cosham and Kirkwood, 2000), e.g. a farmer accidentally gouging a pipeline or a boat denting an offshore pipeline by dragging an anchor across it. The main defects considered in the pipeline are listed as below.

- i. Corrosion
- ii. Gouges
- iii. Dents
- iv. Third-party defects

2.4.1 Corrosion

Corrosion is an electrochemical process. It is a time dependent mechanism and depends on the local environment within or adjacent to the pipeline (Cosham, Hopkins and Macdonald, 2007). NACE International (NACE) states that corrosion is the deterioration of a material, usually a metal, which results from a reaction with its

environment. Corrosion usual appears as either general corrosion or localized (pitting) corrosion. Corrosion causes metal loss. In regards to external corrosion, the environment would be groundwater or moist for onshore pipelines and seawater for offshore pipelines. Figure 2.3 shows the corroded pipeline. For internal corrosion, the environment would be water containing sodium chloride (salt), hydrogen sulphide, and/or carbon dioxide (Baker, 2008). Data for onshore gas transmission pipelines in Western Europe in the period from 1970 to 1997 indicates that 17% of all incidents resulting in a loss of gas were due to corrosion (Cosham, Hopkins and Macdonald, 2007).



Figure 2.3: Corroded pipeline

Source: David Daring

2.4.2 Dents and Gouges

A pipe can be mechanically damaged during transport, construction, while in service, or during maintenance. Mechanical damage can take the form of accidental bends, buckles (surface ripples), dents (deformation of the cross section), gouges (sharp, knife like groove), or fatigue failure (Antaki, 2005). A gouge normally results in a highly deformed, work hardened surface layer and may involve metal removal as shown in Figure 2.4. These damages can result in immediate failure of the pipe, delayed failure or no failure over the design life of the pipeline (Panetta et al., 2001). A dent in a